APPLICATION OF THE EARTH'S FIELD FREE PRECESSION TECHNIQUE IN MEASURING TEMPERATURE DEPENDENT PROTON RELAXATION TIMES IN A DILUTE PARAMAGNETIC SOLUTION

By

DON EDWARD MITCHELL

Bachelor of Science

Oklahoma State University

Stillwater, Oklahoma

1961

Submitted to the faculty of the Graduate School of
the Oklahoma State University
in partial fulfillment of the requirements
for the degree of
MASTER OF SCIENCE
May, 1964

APPLICATION OF THE EARTH'S FIELD FREE PRECESSION TECHNIQUE IN MEASURING TEMPERATURE DEPENDENT PROTON RELAXATION TIMES IN A DILUTE PARAMAGNETIC SOLUTION

Thesis Approved:

F. L. Tollak
Thesis Adviser

Thomas G. Hunter

J. H. Boggs
Dean of the Graduate School

ACKNOWLEDGMENT

The author wishes to express his deepest gratitude to Dr. V. L. Pollak for his guidance throughout the execution of this work. Gratitude is also due the Petroleum Research Fund for partial aid to this project, and the Shell Development Corporation for equipment appropriation. A note of thanks is to be given to Richard Slater for his helpful discussion and/or assistance in carrying out certain experimental procedures.

TABLE OF CONTENTS

LIST OF FIGURES

CHAPTER I

INTRODUCTION

This paper describes the experimental determination of the longitudinal relaxation time T_1, and the transverse relaxation time T_2 (1), of protons in a 0.75×10^{-4} molar solution of manganese ions. The relaxation times were studied as a function of temperature from about 10 to 85 degrees Centigrade. Measurements were made with an "earth's field free-precession" type of nuclear magnetic resonance system. Uniqueness of the "earth's field free-precession" technique is brought out by the fact that the system does not use a rotating magnetic field, but relies on a polarizing field to preorient the magnetic moments at right angles to the earth's field. Such a system enabled the measurement of T_1 in a relatively moderate magnetic field of approximately 440 gauss; and T_2 was measurable in a weak field of about 0.5 gauss, namely that of the earth's field. At the writing of this paper, further instrumentation is being investigated to enable the measurement of T_1 and T_2 in various fields from 440 gauss down to the earth's field.

Relatively few people have exploited the research possibilities of the "earth's field free-precession" technique. First evidence of the technique was described by Packard and Varian (2) in 1954. Later work by Elloit and Schumacher (3) involved the observation of the free induction signal from protons in fluorobenzene in the earth's magnetic field. Beats were noted in the signal which were characterized by the nuclear spin-spin coupling of the protons to the fluorine nucleus. Four

years later, Brown and Thompson (4) studied low field precession signals from aqueous ammonium nitrate solutions which revealed a complex beat pattern characterized again by the spin-spin interaction between protons and nuclei of other species. Brown and Thompson (5) also studied a low-field precession signal obtained from two nuclei of spin one-half coupled isotropically.

To date, however, no work has been done in measuring T_1 and T_2 of protons in dilute paramagnetic solutions as a function of temperature in low fields. In 1956, Bloom (6) measured T_2 in the earth's field and T_1 in various fields up to about 500 gauss at three temperatures (5, 25, and 60°C.) for a 0.5×10^{-4} molar solution of $MnCl_2$. Bloom utilized the free precession technique originally described by Packard and Varian. Later Hausser and Laukien (7) investigated T_1 and T_2 as a function of temperature from 0 to 90 degrees Centigrade for a 1.995×10^{-2} molar solution of $MnCl_2$ in a magnetic field of 6,200 gauss. They used a pulse method with a rotating magnetic field described earlier by Laukien (8). Similar work has been done by Bloembergen and Morgan (9) and by Bernheim, and others (10) in high fields using a spin-echo apparatus. Pfeifer (11) determined T_1 as a function of temperature in several high fields, the lowest being 940 gauss. However, no data was given for T_2.

CHAPTER II

THEORY

Theory of Free Spins in Equilibrium

The theory of the earth's-field-free-precession technique can be adequately understood from a classical approach. Consider first the equation of motion of a single spin magnetic moment at equilibrium. Suppose a sample of nuclear moments is placed in an external magnetic field $\vec{B}$ and the system is allowed to come to equilibrium. The classical equation of motion of the magnetic moment of a single spin $\vec{\mu}$ can be written by noting first that $\vec{\mu}$ is not necessarily along $\vec{B}$. Consequently, there exists a torque given by

$$\vec{\tau} = \vec{\mu} \times \vec{B}. \tag{1}$$

However, the torque equals the time rate of change of angular momentum, or

$$\vec{\tau} = d\vec{L}/dt, \tag{2}$$

so that combination of (1) and (2) gives

$$\vec{\mu} \times \vec{B} = d\vec{L}/dt. \tag{3}$$

From the definition of the gyromagnetic ratio $\gamma \equiv \vec{\mu}/\vec{L}$, equation (3) takes the form

$$\vec{\mu} \times \vec{B} = 1/\gamma \; d\vec{\mu}/dt;$$

or,

$$d\vec{\mu}/dt = \gamma(\vec{\mu} \times \vec{B}). \tag{5}$$

Equation (5) is the classical equation of motion for a single nuclear moment in an external magnetic field, and in the absence of any relaxation effects.

The solution of equation (5) will be considered for the special case of the magnetic field $\vec{B}$ being held constant and uniform. The solution corresponds to a precession of $\vec{\mu}$ about $\vec{B}$ at the Larmor precession frequency. To obtain this solution, consider the dot product of $\vec{\mu}$ with each side of equation (5), or

$$\vec{\mu} \cdot d\vec{\mu}/dt = \gamma\vec{\mu} \cdot (\vec{\mu} \times \vec{B}). \tag{6}$$

Cyclic permutation of the right side of equation (6) gives

$$\vec{\mu} \cdot d\vec{\mu}/dt = \gamma B \cdot (\vec{\mu} \times \vec{\mu}). \tag{7}$$

Since the vector product of a vector with itself is identically zero, equation (7), and consequently equation (6) reduce to

$$\vec{\mu} \cdot d\vec{\mu}/dt = 0. \tag{8}$$

Upon inspection, equation (8) may be rewritten in the form

$$1/2\ d(\vec{\mu}\cdot\vec{\mu})/dt = 0. \tag{9}$$

Equation (9) reveals that $|\vec{\mu}|$ is a constant of motion; that is, $|\vec{\mu}|$ is time independent. In addition, equation (5) indicates that $d\vec{\mu}$ is perpendicular to both $\vec{\mu}$ and $\vec{B}$ so that the resulting motion is a precessional one. Again, it should be emphasized that no relaxation mechanism has been included thus far.

If we let $\vec{B} = B\vec{z}$, the equation of motion expressed in component form becomes

$$\begin{aligned} d\mu_x/dt &= \gamma(\mu_y B_z - \mu_z B_y) = \gamma\mu_y B \\ d\mu_y/dt &= \gamma(\mu_z B_x - \mu_x B_z) = -\gamma\mu_x B. \\ d\mu_z/dt &= 0 \end{aligned} \tag{10}$$

Multiplying the second equation above by "i" = $(\sqrt{-1})$, adding the resulting expression to the first equation, and allowing $\mu_t \triangleq \mu_x + i\mu_y$, one obtains

$$d\mu_t/dt = \gamma B(\mu_y - i\mu_x) = -i\gamma B\mu_t. \tag{11}$$

The solution to equation (11) is given by

$$\mu_t(t) = \mu_t(o)e^{-i\gamma Bt}. \tag{12}$$

Hence, the solutions to equations (10) are given by

$$\begin{aligned} \mu_x(t) &= \mu_x(o)\cos(\gamma Bt) \\ \mu_y(t) &= -\mu_y(o)\sin(\gamma Bt) \\ \mu_z(t) &= \mu_z(o) \end{aligned} \tag{13}$$

Thus, a vector of length $|\mu(o)|$ rotates about the z-axis at a frequency

$$\vec{\omega} = -\gamma\vec{B}. \tag{14}$$

The angular frequency $|\omega|$ is called the Larmor precession frequency and is independent of the angle between $\vec{B}$ and $\vec{\mu}$. For protons

$$\frac{\gamma}{2\pi} = \frac{|\omega|}{2\pi\,|\vec{B}|} = 4.26 \times 10^3 \ \frac{\text{cycles per second}}{\text{gauss}}. \tag{15}$$

Definition of Relaxation Times

The previous discussion has been limited to a single spin moment. Let us consider a finite nuclear magnetization $\vec{M}$ to exist at a given moment and investigate the changes which it will undergo due to thermal agitation and the nuclear magnetic interaction. (The magnetization $\vec{M}$, or the magnetic moment per unit volume, obeys the same equation of motion as the magnetic moment $\vec{\mu}$ of a single spin. $\vec{M}$ is defined at any point within the sample as the average over a small region surrounding that point, the region being small enough so that $\vec{B}$ is uniform over it, but large enough to include many spins.)

The dominant part of the total spin energy U is caused by the strong field $\vec{B}$ in the z-direction, and can be written in the form

$$U = -BM_zV,$$

where V is the volume of the sample over which B is considered uniform.

Major changes in the total energy are therefore necessarily due to a change in the z-component of the magnetization; and it will be the thermal perturbations which will be responsible for these changes. The equilibrium value which M_z will approach under the influence of thermal agitation is given by

$$M = \chi H = \chi B/\mu_0, \tag{17}$$

where χ is the magnetic susceptibility and μ_0 is the permittivity of free space. If at any time $M_z \neq M_0$, it will approach this value exponentially with a characteristic time constant T_1, called the "thermal" or "longitudinal" relaxation time. The rate of change of M_z, due to thermal perturbations alone, can be described by the differential equation

$$dM_z/dt = (M_0 - M_z)/T_1, \tag{18}$$

whose solution is given by

$$M_z(t) = M_0[1 - \exp(-t/T_1)]. \tag{19}$$

The fields which are due to neighboring nuclei contribute to the establishment of equilibrium because of their thermal agitation. Nuclear interactions are also of importance for the changes of the other two components M_x and M_y of the magnetization.

Processes in which the total energy of the spin system does not change, and which therefore affect only the components of the magnetization that are transversal to the field are not necessarily due to internuclear forces alone. Inhomogenities of the z-field (the earth's field here) and the presence of other moments, such as those of paramagnetic ions in solution, will cause similar effects.

Using the analogy to the change of the longitudinal component of the magnetization, we assume the change of M_x and M_y to be one of an exponential character, governed by the equations

$$dM_x/dt = -(1/T_2)M_x, \qquad (20)$$
$$dM_y/dt = -(1/T_2)M_y$$

which both have solutions of the form

$$M(t) = M_o \exp(-t/T_2).$$

For more complete discussion of T_1 and T_2, and their mechanisms, the reader is referred to the literature (1, 9, 10, 13).

Conditions for Producing a Precession Signal

To understand how the behavior of $\vec{M}$ is observed, consider at time $t = 0$ a magnetic field $\vec{B}$ making and angle $\Delta\theta$ with $\vec{M}$. Let the angle $\Delta\theta$ be infinitesimally small, so that $\vec{M}$ is essentially parallel to $\vec{B}$. If $\vec{B}$ were time independent, $\vec{M}$ would precess about $\vec{B}$, maintaining $\Delta\theta$ constant. Now allow $\vec{B}$ to rotate through an angle which is a function of time, say $\alpha(t)$, while the magnitude of $\vec{B}$ is held constant. If $d\alpha/dt$ is much greater than the precession frequency $|\omega|$, the M-vector is left behind. This is the condition for "sudden passage." In this case work is done, since the energy changes by an amount

$$\Delta E = MVB(1 - \cos \alpha), \qquad (22)$$

where V is the volume of the sample.

A second type of passage is possible, and is known as the "adiabatic passage." In this case, $\vec{M}$ follows $\vec{B}$, and no work is done; that is, if

$$d\alpha(t)/dt \ll |\omega|, \qquad (23)$$

then $\Delta E = 0$.

The earth's field free-precession technique depends upon the two conditions described above; however, only the "sudden passage" situation was utilized in the experiments described in this paper. Consider a sample which is inserted into a coil whose axis is perpendicular to the

earth's magnetic field. Allowing a current to flow in the coil will give rise to a field B_p that is parallel to the axis of the coil. The polarizing field B_p may be much larger than the earth's field; hence, the resultant field is essentially that of B_p. Vectorially, this situation may be represented as shown in Figure 1.

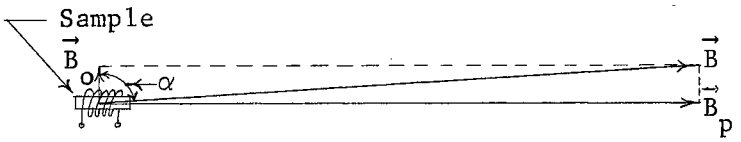

Figure 1. Representation of Magnetic Fields in Earth's Field Magnetometry.

Consider that initially $\vec{M}$ is parallel to the resultant field $\vec{B}$, and has the equilibrium value given by the Curie Law; namely,

$$\vec{M} = N \frac{\mu^2}{3KT} \vec{B} \frac{I+1}{I} \tag{24}$$

where N is the number of nuclei per unit volume, T is the absolute temperature, and I is the spin of the nucleus. If $\vec{B}_p$ is removed suddenly, satisfying the condition for "sudden passage," then the resulting field becomes that of the earth's field $\vec{B}_o$, and $\vec{M}$ precesses about $\vec{B}_o$ inducing a voltage in the coil. The signal is then amplified and observed on an oscilloscope. Note that the same coil is used for initial polarization of the moments in the sample and, upon sudden passage, signal detection.

The condition for sudden passage may be expressed in terms of measurable parameters, $\vec{B}_p$ and $\vec{B}_o$. $\alpha(t)$ is related to $\vec{B}_p$ and $\vec{B}_o$ by the following relation:

$$\tan \alpha = B_p/B_o. \tag{25}$$

Differentiating equation (25) with respect to time such that

$$d(\tan \alpha)/dt = 1/B_o \, (dB_p/dt) = (\sec^2 \alpha) d\alpha/dt, \tag{26}$$

and solving for $d\alpha/dt$, one obtains

$$d\alpha/dt = \cos^2 \alpha/B_o \; dB_p/dt. \tag{27}$$

However, since

$$\omega = \gamma B = \gamma B_o/\cos \alpha, \tag{28}$$

then the condition for sudden passage $d\alpha/dt \gg \omega$ takes on the form

$$\cos^2 \alpha/B_o \; dB_p/dt \gg \gamma B_o/ \cos \alpha, \tag{29}$$

or

$$dB_p/dt \gg \gamma B_o^2/\cos^3 \alpha. \tag{30}$$

This condition must be satisfied during the critical interval in which α is changing; that is, when

$$\frac{1}{10} B_o \leq B_p \leq 10 B_o. \tag{31}$$

Roughly then, the condition $dB_p/dt \gg \gamma B_o^2$ must hold for sudden passage. A calculation finds γB_o^2 to be 7.8 gauss per millisecond if B_o is the earth's field. In practice, however, the rate of change seems to be sufficient if dB_p/dt is approximately fifteen gauss per millisecond.

Calculation of Signal-to-Noise Ratio

Detection of the voltage induced in the coil by the precessing magnetization vector $\vec{M}$ is dependent upon a satisfactory signal to noise ratio. Consider first the calculation of the signal strength. If a strong polarizing field $\vec{B}_p$ is applied to the coil perpendicular to the earth's field $\vec{B}_o$, and the condition that $|\vec{B}|_p \gg |\vec{B}|_o$ prevails, then the magnetization vector $\vec{M}(t)$ is essentially parallel to $\vec{B}_p$. Upon suddenly reducing $\vec{B}_p$ to a magnitude small compared to $\vec{B}_o$, $\vec{M}(t)$ will precess about $\vec{B}_o$ and induce a voltage in the coil proportional to $\vec{M}(t)$. From Faraday's Law (neglecting the sign of the induced voltage for convenience) the

induced voltage is given by

$$E_{pk} = n\,(d\varphi/dt)_{max}, \tag{32}$$

where n is the number of turns (in the ideal case) and φ is the flux due to the precessing magnetic moments. Since the signal is sinusoidal, one may write

$$(d\varphi/dt)_{max} = \omega_o \varphi_{max}; \tag{33}$$

where

$$\varphi = \varphi_{max} \sin \omega_o t, \tag{34}$$

where φ_{max} is proportional to the magnetization $|\vec{M}|$ that has been built up in the presence of $\vec{B}_p$. Without proof one may state that if all the space surrounding the coil is filled with sample, the remanent flux due to the sample after the removal of $\vec{B}_p$ is just χ times the flux associated with $\vec{B}_p$. Combining equations (32) and (33), one may then write for the induced voltage

$$E_{pk} = n\omega_o \varphi_{max} = n\omega_o \chi \varphi_p, \tag{35}$$

where φ_p is the flux of the field $\vec{B}_p$, and χ is the magnetic susceptibility defined by

$$\vec{M} = \chi \vec{H} = \chi \ \vec{B}/\mu_o. \tag{36}$$

Using the relationship $n\varphi = Li$, the peak signal may be expressed in terms of the coil inductance and the polarizing current i_p; that is,

$$E_{pk} = \omega_o \chi i_p L. \tag{37}$$

Since the sample does not occupy all space, it is convenient to introduce the factor η, known as the "filling factor", which is defined as the ratio of the magnetic energy stored in the sample to the total magnetic energy available, or

$$\eta \equiv 1/2 \int B_p^2 dv_s \,/\, 1/2\ Li_p^2, \tag{38}$$

where the integral is taken over the volume of the sample. In view of this, equation (37) then takes on the form

$$E_{pk} = \omega_o \chi i_p L \eta,$$

or,

$$E_{pk} = \frac{\omega_o \chi i_p}{\mu_o} \int \left(\frac{B_p}{i_p}\right)^2 dv_s. \tag{40}$$

Since the receiving coil and the polarizing coil are one in the same, the subscripts on the field to current ratio B_p/i_p may be dropped indicating that B is the field in space for any current i, not necessarily i_p, the applied current. In addition, a factor $\sin^2 \theta$ must be introduced in the integrand of equation (40) to account for the fact that where B_o and B_p are not perpendicular the contribution to the signal is less. Hence, the total expression for the peak induced voltage becomes

$$E_{pk} = \frac{\omega_o \chi i_p}{\mu_o} \int_{sample} (B/i \sin \theta)^2 dv_s, \tag{41}$$

where B/i is the field-to-current ratio at dv_s. If the sample is confined to the center of the coil, the ratio B/i is approximately constant and equation (41) reduces to

$$E_{pk} = \omega_o \chi i_p \, 1/\mu_o \, (B/i)^2 \, v_s, \tag{42}$$

where v_s is the volume of the sample and B/i is evaluated at the center of the coil. The value of the sin θ is unity provided the coil axis is perpendicular to the earth's field.

The signal to the amplifier is picked up across the capacitor in an LC circuit tuned to resonance at the precession frequency ω_o. In such a tuned circuit the signal to the amplifier is given by

$$v_s = \text{signal} = Q \, E_{pk}, \tag{43}$$

where the quality factor $Q = X/R$. At resonance $X = X_L = X_c$. The

resistance R is the a-c resistance of the coil. Hence, the signal, E_{pk} is "amplified" by the Q of the circuit.

The noise voltage generated in the resistance of the coil is given by the Nyquist theorem; that is,

$$v_n^2 = 4KTR\Delta f, \tag{44}$$

where Δf is the bandwidth of the measured noise. The bandwidth may be expressed in terms of the circuit Q:

$$\Delta f = f_o/Q = \frac{\omega_o}{2\pi Q}. \tag{45}$$

In the same manner that the signal voltage was amplified, the circuit Q causes an amplification of the noise voltage:

$$v_n Q = V_n. \tag{46}$$

Thus the noise to the amplifier, as measured across the capacitor in the LC circuit is given by

$$V_n^2 = \left[4KT \frac{X}{Q} \cdot \frac{\omega_o}{2\pi Q}\right] Q^2 = \frac{2}{\pi} KT\omega_o^2 L, \tag{47}$$

where $X = \omega_o L$. Note that the noise voltage to the amplifier is independent of the Q of the circuit.

From equations (42), (43), and (47) the signal-to-noise ratio is therefore given by

$$V_s/V_n = \frac{Q\chi i_p \frac{1}{\mu_o} (B/i)^2 v_s}{[2/\pi\ (KTL)]^{1/2}}. \tag{48}$$

Typical values for a reasonably good coil with a sample volume of about 100 cubic centimeters and a field B_p of approximately 500 gauss give a ratio of about 100/1.

CHAPTER III

THE APPARATUS

Introductory Statements

The apparatus described herein is capable of performing three necessary functions to enable the measurement of relaxation times with the earth's field free-precession technique. The first function is the polarization of the nuclear moments in the sample; the second involves the removal of the polarizing field in accordance with the sudden passage condition (Chapter II); and the third, is the detection and amplification of the free precession signal.

The Coils

The heart of the circuitry involved in the system is a coil into which the sample is inserted. This coil is used for both polarization of the nuclear moments in the sample and detection of the precession signal. The configuration of the coil, as shown in Figure 2, is a slight modification from that of a straight multilayered solenoid. Additional windings are included at each end of the coil to restore the flux density near the ends to that at the center. Figure 3 illustrates the field to current ratio for a constant current as a function of distance along the axis of the coil. The results shown were obtained by inducing a voltage in a search coil of known turns and dimensions placed on the axis of the polarizing coil. The induced

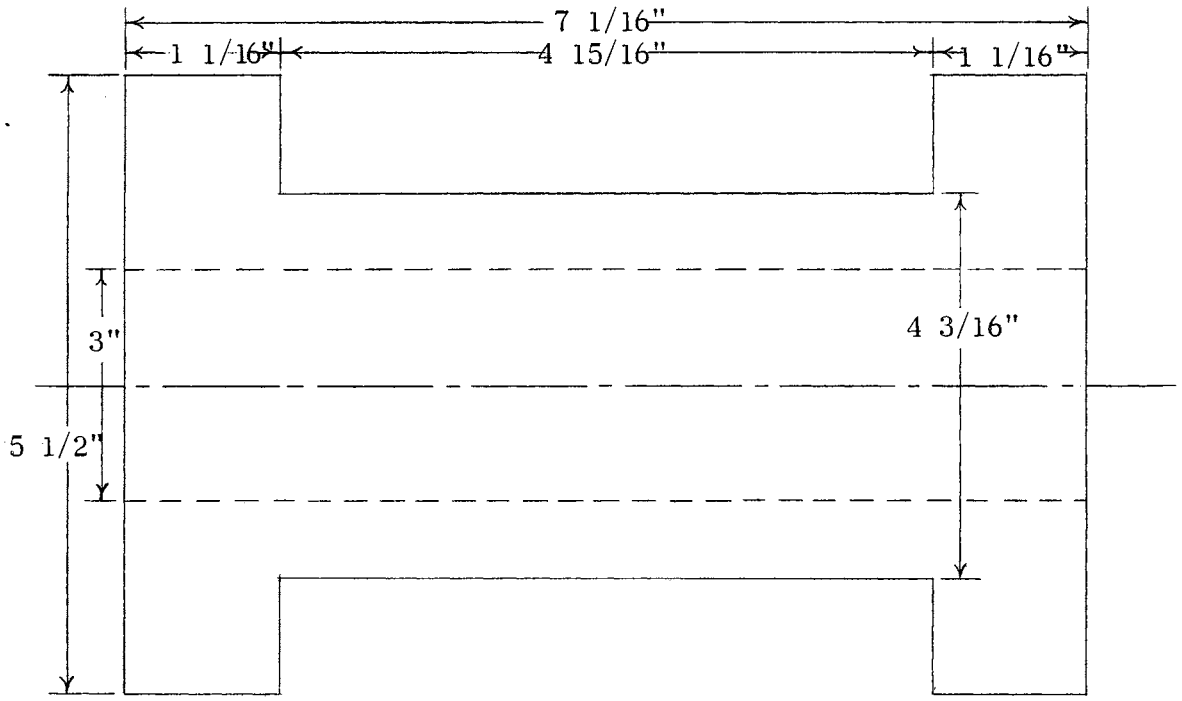

Figure 2. The Sample Coil.

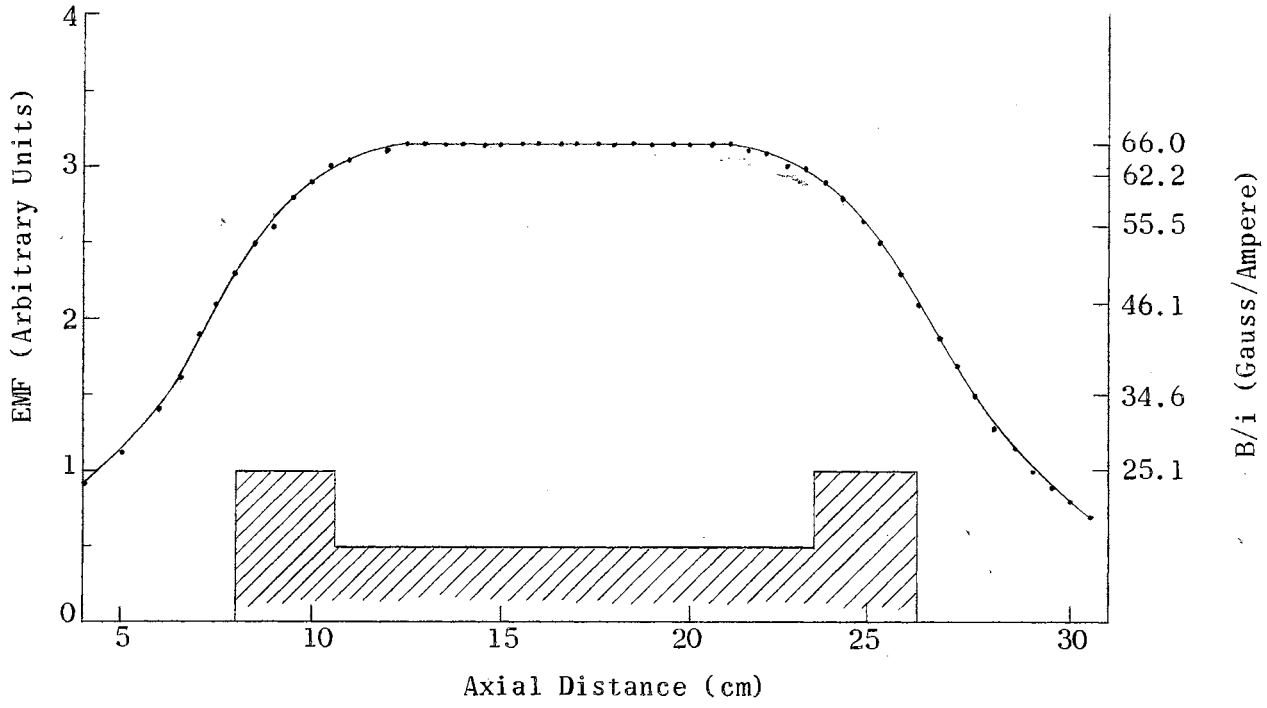

Figure 3. Field-to-Current Ratio Along Axis of Sample Coil.

voltage is a consequence of a sinusoidally varying magnetic field resulting from a known sinusoidally varying current in the polarizing coil.

The field to current ratio was calculated from the relation

$$B/i = E_0/NA\omega, \tag{49}$$

where N is the number of turns in the search coil, A its cross sectional area, and ω the angular frequency of the sinusoidal voltage. At the center of the polarizing coil the field to current ratio was found to be 60 gauss per ampere.

Another calculation for the field to current ratio is obtainable with the relation

$$B/i = \mu_0 N(\cos \alpha)/l \tag{50}$$

where N is the number of turns in the <u>polarizing</u> coil, and l is the length of the coil. The angle α is shown in Figure 4. Using the actual dimensions of the coil (Figure 2) equation (50) gives a value of

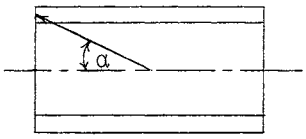

Figure 4. The Angle α of Equation (45).

58 gauss per ampere at the center of the middle coil; that is, excluding the end sections, so that N is approximately 720 turns.

Direct measurement of the field to current ratio has been made with two commercial gaussmeters. A Dyna-Empire Gaussmeter (Model 900) indicated an average value of 69.5 gauss per ampere, while a Bell (Model 300) Gaussmeter indicated an average value of 76.6 gauss per ampere. As a result, an over-all average of 66 gauss per ampere has

been used for the field to current ratio throughout the experiments.

Electrical characteristics of the coil are crucial for the discussion of the complete system and will, therefore, be mentioned at this point. These parameters involve the self-resonant frequency, the inductance, the d-c resistance, and the power consumption for a given current.

In view of the fact that the coil is not a pure inductor due to inherent resistance in the wire and interwinding capacitance, the equivalent circuit may be drawn as shown in Figure 5. By connecting the coil across the output of an oscillator and observing the response with an oscilloscope as a function of frequency, the self-resonant frequency of the coil has been found to be about 35,000 cycles per second.

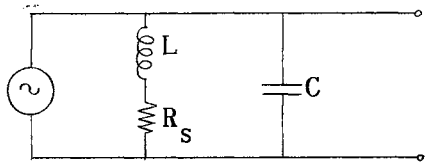

Figure 5. Equivalent Circuit of the Coil.

Measurement of the inductance of the coil was achieved with a parallel LC circuit tuned to about 2,400 cycles per second. Using a known capacitance in the circuit, the inducatnce could be calculated, and was found to be 57.6 millihenrys. An independent measurement with a General Radio Impedance Bridge indicated a value of 58 millihenrys for the inductance of the coil.

These measured values agree fairly well with a value of 38.6 millihenrys for a straight solenoid of the same number of turns and over-all dimensions. The calculation was made for preliminary design of the coil, and involved standard formulas which are available in the Radio

Engineers' Handbook by Terman (15).

The d-c resistance of the coil is 3.450 ohms as measured on a standard Wheatstone bridge. This is in good agreement with a calculated value of 3.44 ohms obtained for the A.W.G. #14 wire used in the coil. Consequently, the power consumed in the coil due to this resistance is about 150 watts for a current of 6.67 amperes. This current gives rise to a polarizing field of about 440 gauss, and is provided by two 12-volt batteries in series.

Current Control

The device for controlling the current in the coil is shown in a simplified circuit diagram in Figure 6. Operation of the switch is understood by considering the voltage and current waveforms as functions of time at the point marked (Y) in Figure 6. These waveforms are illustrated in Figure 7.

At time t = 0 (point 1 in Figure 7) a pulse is initiated to the gate of the first silicon control rectifier (SCR #1) which allows the rectifier to conduct. Consequently, the voltage at (Y) drops to about -23 volts (allowing for a one-volt drop across the conducting SCR) and the current begins to rise toward its quiescent value with time constant L/r, where r is the d-c resistance of the coil, and L its inductance. After some predetermined time interval, depending on the experiment involved, a second pulse is fed to SCR #2 allowing it to conduct. The voltage at (Y) then drops further to about -114 volts (point 2 of Figure 6) and the current and voltage begin to vary sinusoidally due to the now existing RLC series circuit. The capacitor C is large enough so that SCR #1 is kept back biased for a time t_o that is longer than the

recovery time of the SCR, which is about 30 microseconds. At point (3) SCR #1 has been cut off and the voltage and current at (Y) continue to vary sinusoidally, the voltage increasing while the current decreases slightly. When the voltage reaches about 200 volts (point 4), the Zener diode begins conducting resulting in a constant voltage across the coil. The current then decays with time constant L/r at a rate V_z/L, assuming Ldi/dt is large compared to ir. The blocking diode D provides protection from a short circuit across the coil during polarization. When the current has decreased below about 5 milliamperes, the Zener ceases to conduct and the voltage drops back to zero (point 6). In addition, SCR #2 is shut off when the current decreases to a point such that the slight current leakage through r_1 is below the holding current of the SCR.

The rate at which the current in the coil decreases to zero, which is controlled by the Zener voltage, must satisfy the sudden passage condition. This requires that

$$dB_p/dt \gg \gamma B_o^2. \tag{51}$$

If B_p decreases to zero in a time t', then equation (51) may be written in the form

$$t' \ll B_p/\gamma B_o^2, \tag{52}$$

assuming time t = 0 when the voltage first reaches the breakdown voltage of the Zener diode. For a current of 23/3.45, or 6.67 amperes, B_p is about 440 gauss (using a field to current ratio of 66 gauss per ampere). The gyromagnetic ratio for protons is about 2.7×10^4, and the earth's field is about 0.55 gauss. Hence, equation (52) implies that the current must reach zero in a time short compared to 49.4 milliseconds. For a

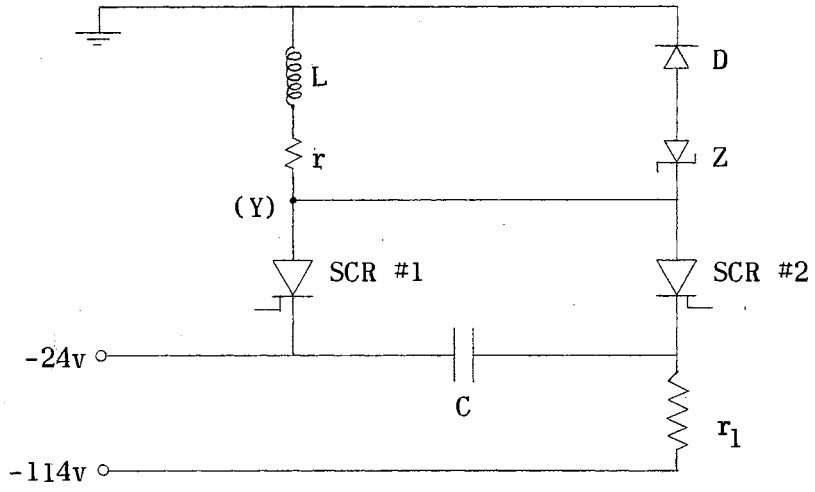

Figure 6. Current Control Device.

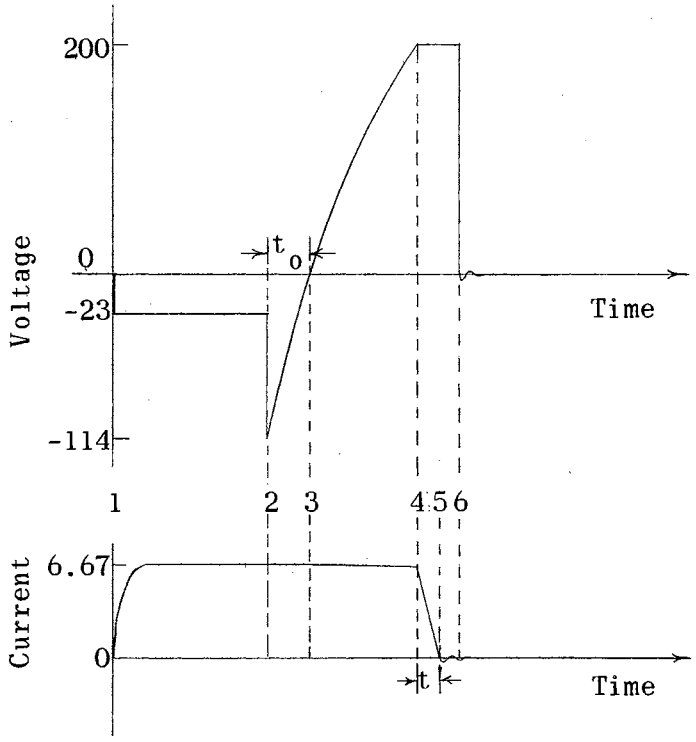

Figure 7. Voltage Current Waveforms at Point (Y) of Figure 6.

Zener voltage of 200 volts, t' is about 1.9 milliseconds, which is certainly sufficient for sudden passage. From observation of the previously described current waveform on the oscilloscope, the cutoff time has been found to be about 1.5 milliseconds. This small discrepancy from the calculated value arises from the approximation that Ldi/dt is much greater than ir.

Detection and Amplification of the Precession Signal

Once the current, and hence, the polarizing field has been removed with sufficient speed, the magnetization vector precesses freely about the earth's field and induces a voltage in the coil. It is now necessary to detect and amplify this signal in order to display the precession signal on an oscilloscope. The fundamental parts of the circuitry for accomplishing detection are shown in Figure 8 along with the switching circuit for clarification.

The relays R_1 and R_2, shown in Figure 8, provide for isolation of the detection circuit from the remaining circuitry during the polarization mode; and reciprocially, during the detection mode, the SCR switching circuit is isolated from the detection system. During the polarizing mode, both relays are energized; they are deactivated only in the detection mode, thus minimizing any additional stray pickup that may exist in the relay activating coils. Relay R_1 is a single pole-double throw Potter and Brumfield Mercury-wetted contact relay (Type JM1-109-12), and relay R_2 is a double pole-double-throw Elgin Crystal Can Microminature Advance relay (#VR/2C/675/D-33). The relay coils are connected as shown in Figure 9. The triggering circuitry for the relays is provided by a standard bi-stable multivibrator (circuit not shown).

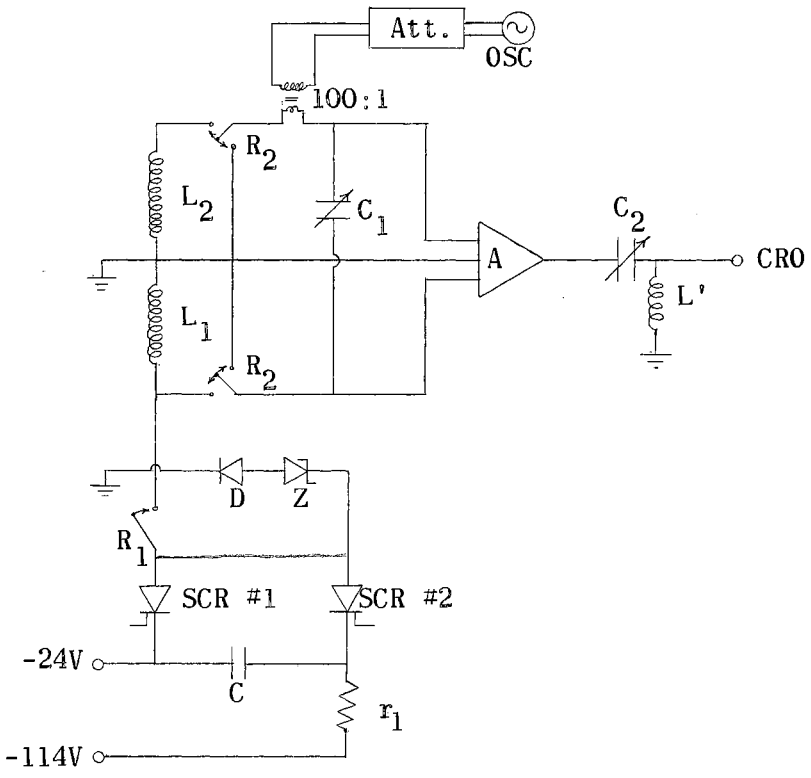

Figure 8. Detection Circuitry.

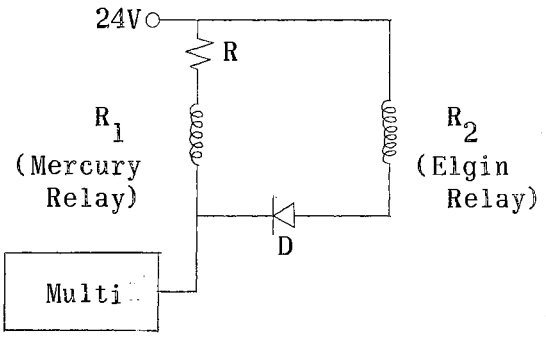

Figure 9. Relay Coil Connection.

The sequence of operation of the relays controls the change from the polarization mode to the detection mode with carefully controlled switching times. At time t = 0, corresponding to the beginning of an experiment, a pulse is fed to the multivibrator causing it to change states. At this time current is allowed to flow through the relay coils. After the relay coils are activated, a time lag persists before the relays actually make contact. For the Mercury relay, this time is about 5.0 milliseconds, and is 4.4 milliseconds for the Elgin relay. Consequently, the pulse fed to SCR #1 cannot be initiated until 5 milliseconds after the initial triggering of the relays.

The relays remain activated until a pulse is fed to SCR #2, initiating the sudden passage turn-off sequence. The same pulse is used to switch the multivibrator to the "off" state, thus removing the activating current to the relays. However, it requires 3.0 milliseconds for the Mercury relay to actually break contact. Since the current in the sample coil L_1 decreases to a very low value in less than 1.5 milliseconds, the contacts of the Mercury relay are not harmed before they break contact. In addition, the Elgin relay requires at least 4.0 milliseconds before making contact on deactivating. This time is longer than the "break time" of the Mercury relay, so that the SCR switching circuit is isolated before the detection circuit is completed, and yet in a time very short compared to the time the precession signal persists. However, for a short duration of about 10 milliseconds after the detection circuit is closed a transient, due to the ringing of the tuned circuit, will mask the actual precession signal. This transient persists for only a short time and is of little consequence.

The above discussion concerning the sequence of operation of the

SCR switching circuit and the relay action may be summarized with the aid of Figure 10. The pulses fed to the gates of each SCR and the multivibrator are supplied by two Tektronix (Type 163) pulse generators. The pulse generators are triggered at appropriate times along the ramp of a sawtooth waveform provided by a Tektronix (Type 162) waveform generator.

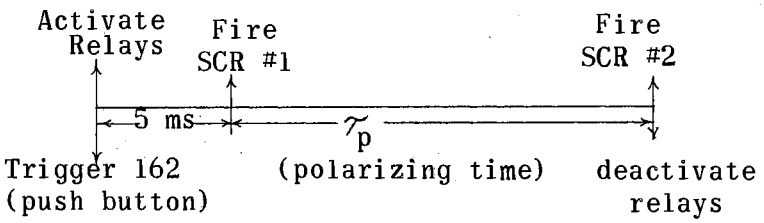

Figure 10. Sequence of Operation of Switching Circuits.

Referring again to Figure 8, it is to be noted that the detection circuit contains two coils, L_1 and L_2. The coil L_1 is the sample coil discussed previously. The coil L_2 is the "bucking" coil, and is (to a close approximation) an exact duplicate of the sample coil. The bucking coil has the same configuration and dimensions as L_1; its inductance is 54.5 millihenrys, and it has a d-c resistance of 3.342 ohms. In the ideal situation, where both coils are identical in every respect, any stray pickup will be cancelled by the second, provided the two coils are connected so as to oppose one another. Thus, only voltages in one coil that are not present in the other will be seen, such as the voltage induced by the precessing moments in the sample coil L_1.

The remaining input circuit to the amplifier, aside from the oscillator-attenuator network, is a parallel LC network capable of being tuned to the precession frequency (about 2,400 cps). The oscillator-attenuator network provides a means of simulating actual signal conditions by allowing a signal to leak in from the oscillator with proper attenuation and frequency. The network consists of a Hewlett-Packard 200CD oscillator

with a Tektronix 170 ohm attenuator across the output. Attenuation ranges from 1 to 64 decibels. An additional 40 decibel attenuation is achieved with a step down transformer provided by a Triad 100 millihenry torroid for the primary, and 8 turns of A.W.G. #30 wire for the secondary. The available attenuation has been found to be within two per cent of the rated values, the existing discrepancy being due to slight impedance mismatching. Consequently, a signal of known amplitude can be fed into the circuit such that the voltage seen at the output becomes a measure of the gain, or Q, of the circuit. Such a measurement at the output of the parallel LC circuit indicated a Q of 25.

An alternative technique for measuring the Q of a tuned parallel circuit makes use of the bandwidth of the frequency response. The bandwidth is $2(f_i - f_o)$, where f_o is the resonant frequency and f_i is the frequency off resonance such that the response is 3 decibels below the response at resonance. The Q is then $f_o/(f_i - f_o)$, or $f_o/(bw)$. Using this technique, the Q of the input circuit was found to be 25.9.

Since any ferromagnetic material contributes to the non-uniformity of the earth's field, the coils had to be placed in an area where such material was at a minimum. Consequently, the coils were connected at one end of a 90 foot long cable and the remaining circuits and instruments at the other end. Introduction of this cable into the circuitry caused appreciable drop in the Q of the input circuit. Measurement of the ratio of the voltage produced at the output to that leaked into the input circuit indicated a Q of 17.5. The 3-decibel method showed the Q to be 18.9.

This drop in Q has been attributed to losses in the cable dielectric which was noted to be a low grade of rubber. The capacitance between

the cable conductors which carry current was measured to be 3389 pico-farads. The dissipation factor was also measured for the dielectric between these conductors and found to be 0.0622.

The amplifier shown in Figure 8 is a Tektronix low-level Type 122 preamplifier with a differential balance control in the cathode of the first push-pull stage, which permits adjustment for the best possible rejection of in-phase signals. The maximum open circuit gain is rated at 1,000; however, the gain measured with the d-c level control fully counterclockwise was found to be about 970.

The output tuner in Figure 8 is essentially a high pass filter, but with a high peak response near 2,400 cycles per second. Consequently, it is treated as a band-pass filter with a bandwidth of about 180 cycles per second. The band-pass is nonsymmetrical, being slightly skewed toward frequencies above the peak response frequency. Gain of the tuner, or Q, is about 19, and the addition of this network at the output of the amplifier causes the amplifier gain to drop to about half its unloaded value, namely about 491. The a-c resistance of the tuner was found to be about 900 ohms, which is close to the measured output impedance of the amplifier gain to about half its unloaded value.

The gain of the complete system is about 168,000 with a bandwidth at the output of approximately 100 cycles per second. Hence, a signal of only 3 microvolts generated by the precessing magnetization vector will be amplified to a signal of 500 millivolts at the output of the system. However, any thermal noise generated in the coils will also be amplified accordingly, in addition to noise contributions from the amplifier itself.

The thermal noise can be calculated from equation (47) of Chapter II:

$$V_n^2 = \frac{2}{\pi} KT\omega_o^2 L(1.57) \qquad (47a)$$

where the factor 1.57 has now been included to account for the fact that the band-pass is not square. Equation (47a) can be rewritten in the form

$$V_n^2 = 4KTfX_L(1.57). \qquad (53)$$

Calculation of the noise voltage in the input tuning circuit indicates that there will appear a noise voltage of 0.33 microvolts (rms) at the amplifier input, or about 3 millivolts (rms) at the final output of the system. Amplifier noise is neglected in this calculation.

Measurement of the noise of the system indicates a 10 millivolt (0 to peak) noise with contributions being amplifier noise, thermal noise of the input circuit, and 60 cycle harmonics. The amplifier noise, measured with short circuit input, was found to be approximately 5 millivolts (0 to peak) with negligible 60 cycle contributions. Consequently, about 2 millivolts of noise were contributions from thermal noise and 60 cycle harmonics in the band-pass. Most of the 60 cycle pickup can be eliminated with proper alignment of the coils.

System Tuning and Signal-to-Noise Measurement

Final checkout of the complete system was made with a sample of tap water. Once a precession signal was obtained, it was necessary to "tune" the system. This tuning of the system must be done at the beginning of each experiment where different samples and locations are involved. The tuning procedure requires the measurement of the precession frequency, and the adjustment of the capacitors to peak the response of the system at the precession frequency.

Measurement of the precession frequency is accomplished by allowing

a signal to leak into the system from the oscillator, superimposed upon the precession signal. The oscillator frequency is then varied until the beating of the two signals ceases. The frequency at which this occurs is the Larmor precession frequency for the nuclear moments concerned. Actual measurement of the oscillator frequency is then made with a Hewlett-Packard (Model 522B) electronic counter. The precession frequency in this vicinity was found to be about 2310 cycles per second, indicating an earth's field strength of 0.542 gauss. Once the oscillator is set to the precession frequency, the tuning capacitors are then adjusted until the observed response is a maximum.

Measurement of the actual precession signal amplitude is accomplished by adjusting the amplitude of the oscillator output until the observed signal coincides with the initial amplitude of the precession signal. The actual output voltage of the oscillator times the noted attenuation to the input circuit gives the amplitude of the precession signal. For a fully polarized water sample 500 cubic centimeters in volume, a 6.65 microvolt (0 to peak) signal was observed. This agrees well with a calculated 5.75 microvolt (0 to peak) signal obtained from equation (42). Consequently, with an over-all system gain of 168,000, a signal-to-noise ratio of 112 is obtainable with a 500 milliliter sample.

CHAPTER IV

SAMPLES, EXPERIMENTAL METHODS AND DATA REDUCTION TECHNIQUES

Introductory Statements

Attention is now given to the preparation of the samples investigated, experimental techniques, and methods of data reduction for determining relaxation times. In addition, methods of controlling the temperature of the samples, and problems encountered in the procurement of data are presented in this chapter.

Preparation of the $MnCl_2$ Solution

The aqueous solution of paramagnetic ions investigated contained 4.5×10^{16} manganese ions per cubic centimeter, and was obtained with a 0.75×10^{-4} molar solution of $MnCl_2$. This concentration was desirable in that the solution is characterized by a transverse relaxation time of about 200 milliseconds at room temperature. A T_2 of 200 milliseconds is short enough that the contribution of relaxation due to the earth's field gradient can be neglected, and yet long compared to the ringing time of the tuned input circuit and associated switching transients.

Preparation of the solution of desired concentration was accomplished two ways. The first method involved actual weighing of a desired amount of $MnCl_2$ crystals to be placed in solution. The accuracy of this procedure proved doubtful; and consequently, the resultant solution was

used only for preliminary studies to gain familiarity with the technique of making relaxation time measurements. The uncertainity in the accuracy of the concentration arose from the fact that the only reagent form of $MnCl_2$ available was $MnCl_2 \cdot 4H_2O$. The reagent appeared aged; and since the salt is deliquescent, it was suspected that more than four waters of hydration were associated with each $MnCl_2$ molecule. A simple calculation shows that one additional water of hydration per $MnCl_2$ molecule introduces a 9% error in the concentration of the final solution.

However, a one liter solution of aqueous $MnCl_2$ was prepared from the available crystals under the assumption that the given chemical composition of the reagent, $MnCl_2 \cdot 4H_2O$, was correct. For a one liter solution, 14.95 milligrams of the reagent salt were required to obtain a molar concentration of 0.75×10^{-4}. The crystals were weighed on an analytical balance, the measurement being correct to one tenth of a milligram. In addition, the measured volume of the solution was correct to the nearest 10 milliliters, or 1%. If the given composition of the reagent was correct, the final concentration could be depended upon to be correct to within 2%. Relaxation time measurement of the solution indicated a T_2 of 235 milliseconds ± 10 milliseconds at 25 degrees Centigrade. Hence, the solution was useful for preliminary measurements.

A second, more dependable solution was prepared from a titration for the chlorine ion with a silver nitrate solution of known molarity. Since silver nitrate crystals are not deliquescent, the difficulty in the previous method of direct weighing was eliminated. A 250 milliliter solution of aqueous silver nitrate was, therefore, prepared by the previous technique for a 0.0937 molar concentration. The concentration

was accurate to less than 1%. In addition, a 250 milliliter solution of $MnCl_2$ with a molar concentration of approximately 0.04 was similarly prepared. At the titration end point

$$\text{(volume of } AgNO_3 \text{ solution used)(moles of } AgNO_3\text{/liter)} = 2\text{(volume of } MnCl_2 \text{ solution used)(moles of } MnCl_2\text{/liter)}. \quad (54)$$

Upon reaching the desired end point, the above calculation indicated a molarity for the $MnCl_2$ solution of 0.0498. Another independent titration using a 0.0506 molar solution of $AgNO_3$ indicated a molar concentration of 0.0484 for the same $MnCl_2$ solution. These two results are within 3% of each other, the difference being attributed to the determination of the exact end point inthe two titrations. The final concentration of 0.75×10^{-4} molar was then obtained by diluting a small, carefully measured amount of the prepared "standard" solution with distilled water.

Method of Determining T_2

As discussed previously, the observed transverse relaxation time T_2 is defined as the time constant of the exponential decay of the component of the magnetization vector perpendicular to the static field. The signal observed is characteristic of the relaxation toward a state of thermodynamic equiliblium in which the magnetization vector ends up aligned with the earth's field. This is the result of prepolarization of the magnetization vector perpendicular to the earth's field. In turn, prepolarization is a consequence of relaxation toward another state of thermodynamic equilibrium characterized by T_1, which will be discussed momentarily. The transverse relaxation time T_2 is then the

time constant of the observed exponentially decaying signal.

In principle, the simplest method for determining the time constant of the observed exponential envelope is to measure the time required for the amplitude of the signal to decay to 1/e of its original value. However, this method is difficult due to the short time that the signal is visible on the oscilloscope screen. The oscilloscope used in these experiments is a Tektronix (Type 535 A) with a high gain differential preamplifier (Type D) plug-in unit. The instrument is equipped with a delayed sweep mechanism which allows the sweep to be delayed for a controlled time interval after the initial triggering of the oscilloscope. In this mode of operation, only that part of the signal subsequent to the decay time is observed on the screen. Hence, by varying the delay time, accurate measurements can be made of the signal amplitude as a function of time. From these measurements, the decaying signal may be reproduced graphically.

The equation of a decaying exponential curve is given by

$$E(t) = E_0 \exp(-t/T_2), \tag{55}$$

where T_2 is the time constant of the curve. Consequently, T_2 is given by

$$T_2 = t/\ln[E_0/E(t)]. \tag{56}$$

In practice, it was convenient to plot the curve on a semi-log scale. The exponential could then be drawn with a straight line through the scatter of data points. This eliminates the difficulty encountered in trying to construct an exponential curve between data points plotted on a linear scale. The slope of the straight line on the semi-log plot is then $1/T_2$. In addition, the semi-log plot gave some indication as to whether or not the decaying signal was truly exponential.

Method of Determining T_1

It has been pointed out in Chapter II that the longitudinal relaxation time T_1 is defined as the time constant of the exponential growth of the component of the magnetization vector parallel to the static field. The static field in this case is the polarizing field B_p, which is 420 gauss in these experiments. Determination of the relaxation time involves the measurement of the amplitude of the precession signal as a function of the polarizing time τ_p. Variation of the polarizing time is accomplished by changing the point at which the second pulse generator is triggered. It is the pulse of the second pulse generator which initiates the fast turn-off sequence described in Chapter III. The time interval τ_p is measured with the Hewlett-Packard electronic counter.

Since the oscilloscope is initially triggered at the beginning of the fast turn-off sequence, the signal observed includes the transients inherent in switching to the detection mode (see Chapter III), which last about 20 milliseconds. Although not necessary, it was found convenient to again make use of the oscilloscope's time delay mode of operation; that is, the sweep was delayed 20 milliseconds after the initial triggering of the oscilloscope. Consequently, only the free precession signal subsequent to these transients was observed on the oscilloscope screen.

The longitudinal relaxation time is then the time constant of the exponential curve obtained by plotting signal amplitude as a function of the polarizing time. For reasons discussed at the end of this chapter concerning the control of the temperature of the sample, the polarizing time was usually not increased enough to allow full polarization of the magnetization vector. Also, since the calculation of the time constant

of an increasing exponential requires knowledge of the signal amplitude at full polarization (equilibrium), the semi-log plot discussed earlier is inadequate unless the value of the amplitude at full polarization can be found. However, an alternate graphical method exists which provides not only the amplitude at equilibrium, but T_1 itself.

Consider the equation of an increasing exponential with time constant T_1. Such an equation is given by

$$E(t) = E_0[1 - \exp(-t/T_1)], \tag{57}$$

where E_0 is the signal amplitude at full polarization. At some τ seconds later,

$$E(t + \tau) = E_0\{1 - \exp[-(t + \tau)/T_1]\}. \tag{58}$$

The time interval τ is usually chosen to be on the order of one time constant. Substituting equation (57) into (58), and with a little albegra, it can be shown that

$$E(t + \tau) = E_0[1 - \exp(-\tau/T_1)] + E(t)\exp(-\tau/T_1). \tag{59}$$

Equation (59) is the equation for a straight line with independent variable $E(t)$, dependent variable $E(t + \tau)$, slope $m = \exp(-\tau/T_1)$, and intercept $b = E_0[1 - \exp(-\tau/T_1)]$. The intersection of this line with a straight line of slope $m = 1$ and passing through the origin is E_0. This fact can be shown by noting that at the intersection of these two lines $E(t) = E(t + \tau)$. Substituting $E(t)$ for $E(t + \tau)$ into equation (59) and solving for $E(t)$ indicates that

$$E(t) = E[1 - \exp(-\tau/T_1)] + E(t)\exp(-\tau/T_1). \tag{60}$$

Solving for $E(t)$ shows that $E(t) = E_0$. By measuring the slope m of the curve for $E(t + \tau)$, the relaxation time T_1 may be calculated from the equation

$$T_1 = -\tau/\ln(m). \tag{61}$$

Hence, at least two graphs are necessary in order to determine T_1. The first is a plot of the raw data; that is, a plot of the signal amplitude E(t) as a function of the polarizing time τ_p. From this curve, a reasonable value of τ is chosen, and a second plot of E(t) versus $E(t + \tau)$ constructed. The relaxation time may either be calculated from the slope of the straight line in the second graph; or a third; semi-log plot of $E_o - E(t)$ versus τ_p may be constructed from which T_1 can be calculated from the equation

$$T_1 = \tau_p / \ln[E_o/E_o - E(t)]. \tag{62}$$

Water Corrections

The above procedures in data reduction had to be carried one step further to obtain the desired final result. A small, but significant, correction for the intrinsic relaxation of the water was necessary. Intrinsic relaxation of the water itself is a subtle point in the present experiments, since it is used here to account for all contributions to relaxation other than that of the manganese impurities. Such effects include primarily relaxation due to small amounts of dissolved paramagnetic oxygen, and, in the case of T_2, field inhomogenities. However, by repeating the experiments with a sample of water that did not contain manganese ions, all these effects could be lumped together and the proton relaxation due to the manganese impurity alone found using the relation

$$1/T^{Mn} = 1/T^{obs} - 1/T^{H_2O}, \tag{63}$$

where T^{H_2O} indicates the intrinsic relaxation of the water. The relaxation time observed from the solution of $MnCl_2$ is denoted by T^{obs}; and relaxation due to the manganese ions alone is given by T^{Mn}.

It should be emphasized that $T_2^{H_2O}$ may not be characterized by an exponential, thus preventing complete justification for the use of the graphical techniques described earlier. This difficulty arises from the fact that $T_2^{H_2O}$ is longer than T_2^{obs} by more than one order of magnitude, particularly at higher temperatures. Consequently, the effect of the earth's field gradient may play a dominant role in the transverse relaxation, and such a contribution is not known to be characterized by an exponential form of decay. However, graphical analysis obtained from the water data indicated only slight deviation from an exponential. Hence, the analysis was considered justifiable and the correction (63) was used to obtain the desired relaxation times due only to the manganese ions.

Temperature Control

The above procedure for determining T_1 and T_2 must be carried out at each temperature over the range investigated. Control of the temperature throughout the range studied was maintained with an unsilvered Dewar flask that would contain a solution of about 200 milliliters in volume. The mouth of the flask was kept closed with a one-hole neoprene stopper through which a thermometer was inserted. In addition, the flask was wrapped in surgical tape to prevent shattering of the glass in case of breakage, and to provide for some additional insulation. Considerable care had to be taken with regard to the materials used since any magnetic material in the near vicinity of the coils contributed to the non-uniformity of the earth's field. Each material to be used in connection with the Dewar flask was carefully checked for magnetic material by placing the substance inside the coils along with a sample of distilled

water. If any noticeable change in the decay time of the signal from the water occurred as a result of the presence of the foreign material, the material was rejected.

Solutions to be investigated were cooled in a clean Pyrex flask placed in a salt-ice bath. Just prior to the freezing of the solutions, the flask was removed and the material transferred to the Dewar flask. The Dewar was usually not filled completely to allow for some expansion of the solution on heating to room temperature. In a similar manner, the solutions were heated in a Pyrex flask held above a hot plate. Heating was allowed to continue until the temperature was just short of boiling. The solution was then quickly transferred to the Dewar and placed in the coil. The solution was prevented from boiling to minimize any change in the concentration of the solution resulting from evaporation of the solvent upon boiling. A 200 milliliter sample of pure water had been checked for evaporation near the boiling point, and was found to have lost only 4 milliliters out of the original 200. To a close approximation, this causes a change of about 2% in the concentration of a 200 milliliter sample of the $MnCl_2$ solutions that were used.

After the sample had been heated or cooled and placed in the Dewar flask, it was allowed to approach the equilibrium temperature naturally while data was taken. The rate of change of the temperature was high near the extreme temperatures. Consequently, data had to be obtained as quickly as possible between temperature readings. This accounts for the fact that, during T_1 measurements, the polarizing time was usually not increased sufficiently to allow the magnetization to reach equilibrium in the polarizing field. In addition, each set of data obtained for a given temperature was taken twice, the temperature

recorded as the average between that taken before and after the run. Each time the temperature was read, the sample was removed from the coil and lightly shaken to insure a better indication of the temperature throughout the sample. Readings were accurate to the nearest degree and estimated to the nearest half of a degree. When the temperature began to approach the equilibrium temperature more closely, it became necessary to remove the stopper from the Dewar flask and stir the sample for a while before the temperature would change significantly. Ordinarily, data points were obtained practically every 2 degrees in the range from about 10 to 85 degrees Centigrade.

Uncontrollable Problems

Although the above discussion of the technqiues for making relaxation time measurements is relatively straight-forward, several problems were encountered which warrant mention. The most severe problem arose from the reduced signal-to-noise ratio due to the smaller volume of the solution in the Dewar flask. It has been pointed out in Chapter III that a signal-to-noise of 112 was measured with a 500 milliliter sample of water. The samples used in the Dewar were about 150 milliliters in volume. For the same 10 millivolt noise measured previously, a 150 milliliter sample produces a signal-to-noise of only 34. On some days, the noise was seen to increase to almost 20 millivolts; thus causing a further reduction in the signal-to-noise ratio. This increase in noise was mostly due to additional activity of electrical machinery in the area during the daylight hours. Consequently, it was advantageous to make most of the runs during the evening hours. However, the high temperature runs were usually made during the warm

afternoons since the ambient temperature was higher and the rate with which the temperature changed was, therefore, lower.

The increased noise in the daylight hours was found to be primarily 60 cycle harmonics in the band pass. This was evidenced by the fact that the precession signal sometimes appeared slightly modulated, thus causing the observer to integrate the signal by eye to obtain the amplitude at any given instant. This effect may also be partly attributed to the nonuniformity of the earth's field over the volume of the sample since the effect was still present, although to a lesser degree, in the evening hours. Additional problems were encountered when the coils had to be removed from their station due to impending weather conditions. It was naturally impossible to place the coils again in their exact previous position. Consequently, the earth's field gradient was not consistent throughout the entire experiment. However, this difficulty was of small concern.

CHAPTER V

RESULTS AND CONCLUSIONS

Introductory Statements

In this chapter the results of the work described in the preceding chapter will be presented. Additional discussion will be presented concerning various conclusions with regard to these results and to the utility of the apparatus in general. Several suggestions with respect to refinements of the system and areas for further study are also to be given.

Results on T_2

Figures 11 through 18 indicate the behavior of proton relaxation times T_1 and T_2 as functions of temperature. The data obtained for the "observed" transverse relaxation time, T_2^{obs}, of the 0.75×10^{-4} molar $MnCl_2$ solution is shown as a function of temperature in Figure 11. It should be emphasized that the data has not yet been corrected for the intrinsic relaxation of the water. The results indicate a general increase in T_2^{obs} with increasing temperature. The scatter of points is, for the most part, less than 10% throughout the range of temperatures investigated. This was considered exceptionally good considering the loss in signal-to-noise at higher temperatures and the crudeness in the graphical approach to data reduction described earlier.

The data in Figure 12 was obtained from a sample of distilled water

in which manganese ions were not present. The curve obtained was used to correct the data in Figure 11 for the intrinsic relaxation of the solvent in the $MnCl_2$ solution. Since $T_2^{H_2O}$ is, on the average, an order of magnitude longer than T_2^{obs}, the correction is small, and consequently, a straight line was drawn through the scatter of points even though a "double s" curve appeared to be a better fit. As expected, there appears to be a slight increase in the scatter of data for the water sample. The transverse relaxation is longer for the pure water and is, therefore, more susceptible to field gradient contributions which tend to make the signal decay non-exponential. Hence, the plot of the raw data on a semi-log scale assuming an exponential decay introduced obvious error.

Figure 13 is the final plot of T_2 showing the effect of temperature on transverse proton relaxation in the $MnCl_2$ solution after the water correction has been made on the data in Figure 11. The data in Figure 13 was obtained by taking data for the water correction from the straight line in Figure 12 and applying it to each point in Figure 11 at corresponding temperatures using the relation indicated in Chapter IV; that is,

$$1/T_2^{Mn} = 1/T_2^{obs} - 1/T_2^{H_2O}. \tag{64}$$

The effect of the water correction is noted in Figure 13. In addition to the expected general increase in transverse relaxation time, a change in curvature is observed with a decided increases in T_2 at temperatures below ambient.

A plot of the data shown in Figure 13 is reproduced on a different scale in Figure 17 along with experimental results of other workers (6, 9, 10). The product of molar concentration on manganese ions N, and relaxation time T_2, is plotted as a function of reciprocal absolute

temperature on a semi-log scale for convenience of comparison. Not only is the temperature dependence evident, but field dependence is indicated (see legend). More complete information concerning field dependence is shown in Figure 19, and will be discussed later.

The general shape of the curve in Figure 13 is in agreement with other results found in relatively low and moderate mangetic fields. High field results are seen to deviate from this shape at low temperatures due to relaxation mechanisms which are fully discussed in the literature (9, 10). In addition, the experimental results obtained by Bloembergen and Morgan (9) indicate that T_2 decreases with increasing field in the range from 3,300 to 14,100 gauss, which is in good agreement with their proposed theory (9). According to experimental results shown in Figure 19, which indicate the field dependence of NT_2 (and NT_1), there appears good agreement among several workers (6, 9, 10, 11, 12, 14) throughout the range stated above. Morgan and Nolle (14), however, obtained results in lower fields (Figure 19) that indicate a reversal in the field dependence of T_2. Their results imply that T_2 tends to increase with increasing field in the range from about 500 to 1,400 gauss. Examination of the Bloembergen and Morgan theory suggests that such a field dependence exists, and that in the limit of weak fields, T_2 should be nearly a factor of two shorter than it is in moderately high fields of 3,000 gauss. The results in this experiment, and those obtained by Bloom (6) agree fairly well with this suggestion for the earth's field case. No data, however, exists for intermediate fields up to 500 gauss to verify that such a field dependence is indeed the case. A more detailed study of the Bloembergen and Morgan theory is no doubt desirable, but such an endeavor shall not be attempted here.

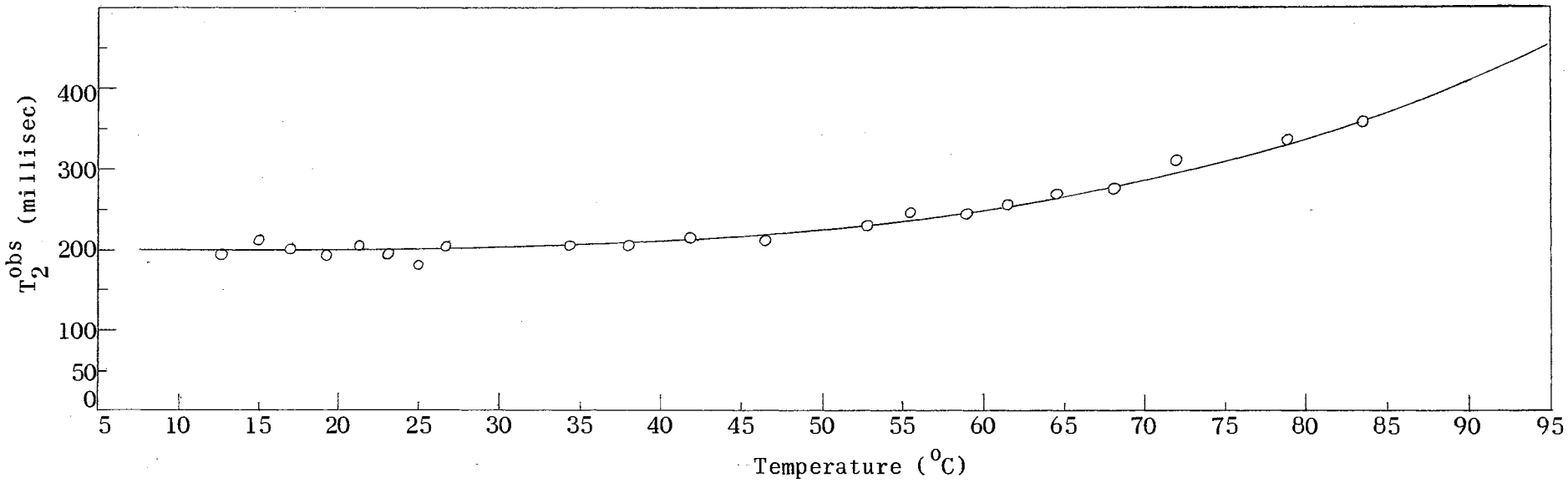

Figure 11. T_2^{obs} vs. Temperature for $MnCl_2$ Solution.

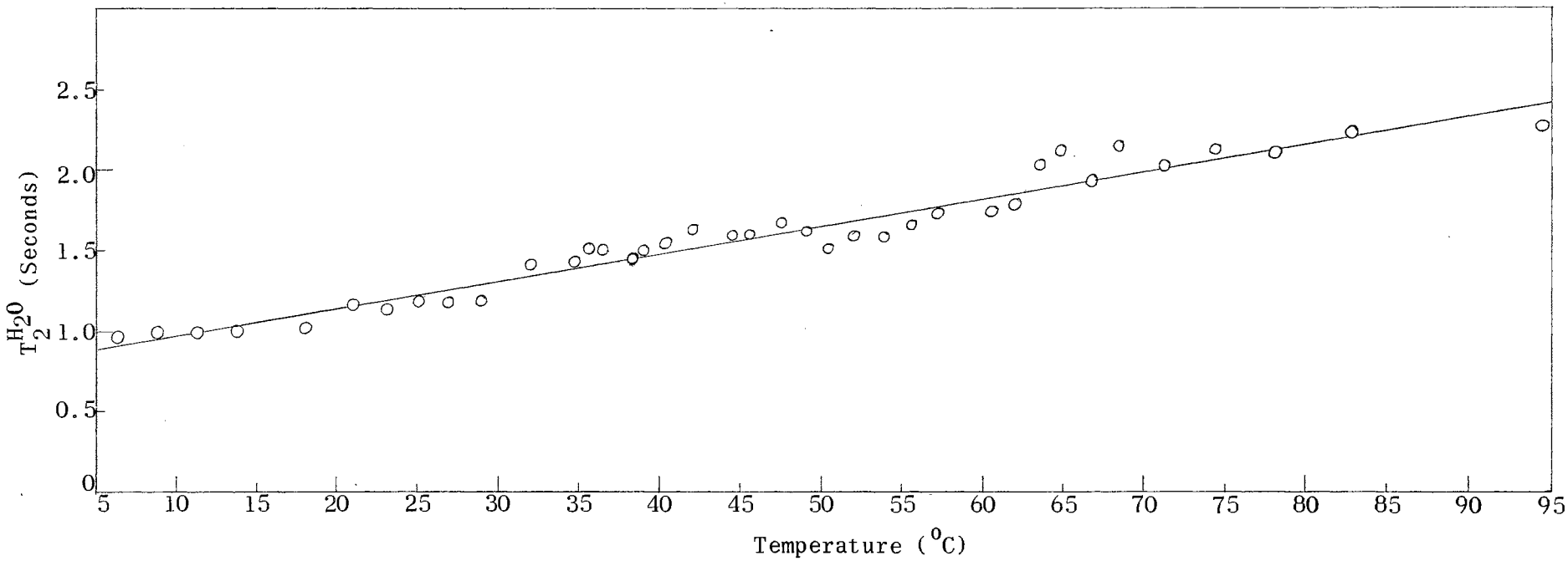

Figure 12. $T_2^{H_2O}$ Temperature for Water.

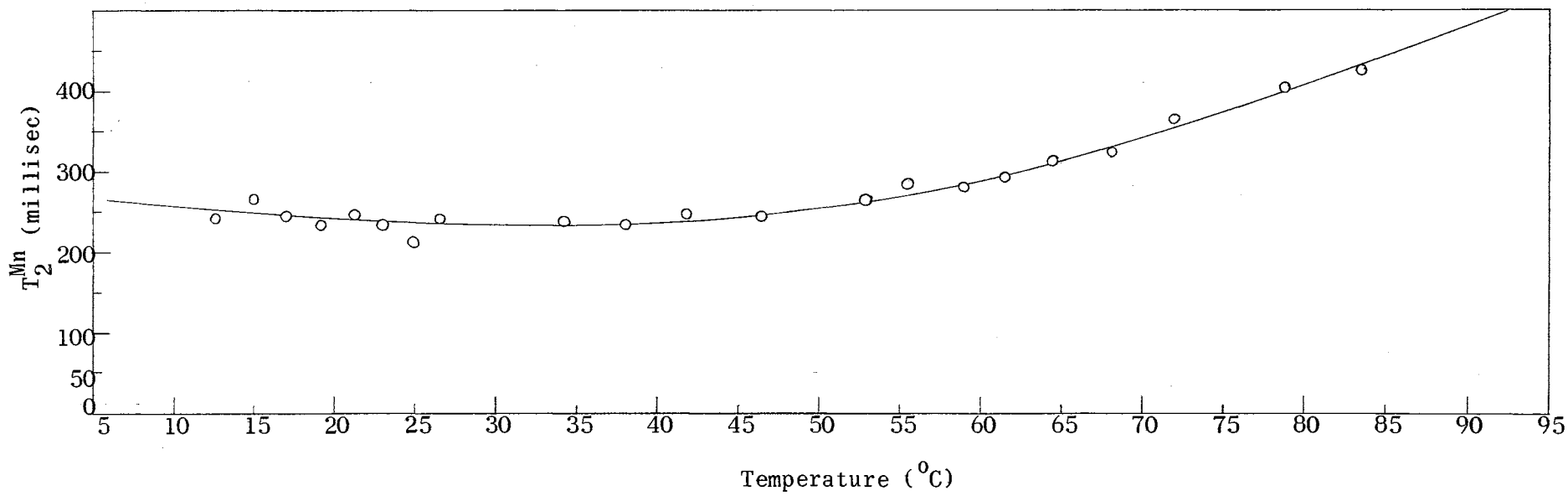

Figure 13. $T_2^{H_2O}$ Temperature for $MnCl_2$ Solution.

Results on T_1

The longitudinal relaxation time T_1^{obs} observed from the $MnCl_2$ solution is shown as a function of temperature in Figure 14. Figure 15 is a similar plot of the data obtained from a pure water sample in which no manganese ions were present. The data in Figure 14 was then corrected in the same manner as previously discussed for the intrinsic relaxation of the water and the results plotted in Figure 16. The only apparent effect of the water correction in this case was the general increase in T_1^{Mn} throughout the temperature range studied.

The most significant point of discussion in the case of the results for T_1 is the unusual scatter at temperatures above ambient in both the data for the $MnCl_2$ solution and the pure water sample. Below room temperature, scatter is on the same order as that noted for the data on T_2. However, an abrupt increase in scatter occurs in all data above room temperature. This cannot be attributed to a loss in signal-to-noise at higher temperatures for two reasons. In the first place, the loss in signal-to-noise at increased temperatures arises from the fact that the signal amplitude is inversely proportional to the temperature. (This fact was mentioned earlier.) However, the same situation occurs in the case of T_2, and as indicated in Figures 11 through 13, very little scatter was observed compared to that noted for data on T_1. Secondly, the effect of decreasing signal-to-noise is one that increases continuously with increasing temperature, which does not account for the abrupt increase in scatter just above the room temperature.

Explanation for this unreasonable scatter has been attributed, consequently, to some aspect of obtaining data in the above ambient

temperature range which differed from that taken below ambient. The answer to this problem still remains uncertain.

Figure 18 is a semi-log plot, similar to that of Figure 17, of NT_1 versus reciprocal absolute temperature, where N is again the molar concentration of the $MnCl_2$ solution. In addition to the data obtained from the present experiments, results of other workers are shown (6, 9, 11). The temperature dependence of NT_1 is seen to agree well with all other reported results indicating a general monatonic increase in relaxation time with increasing temperature. In addition, the field dependence of T_1 is evident from the figure. Results obtained from the experiment, performed in an average magnetic field of 440 gauss, agree relatively well, particularly with regard to the data available from Pfeifer (11) and Bloom (6). The lowest field investigated by Pfeifer was 940 gauss. These results are noted to lie above the data found in this experiment, as expected. Also, data at approximately 130 gauss, found by Bloom, lies below that obtained at 440 gauss.

Further support of the data found at 440 gauss in the present work is shown in Figure 19 where good agreement is also noted with the results obtained by Morgan and Nolle (14), in a field of 470 gauss.

Conclusions and Suggestions for Further Study

This paper has been presented as support for the evidence that the apparatus described herein is useful as a research tool. This evidence supercedes any implications that may be derived from the results concerning the validity of existing theories on mechanisms for relaxation. Such implications undoubtly lend motive to further investigations which utilize the present equipment and/or additional instrumental refinements

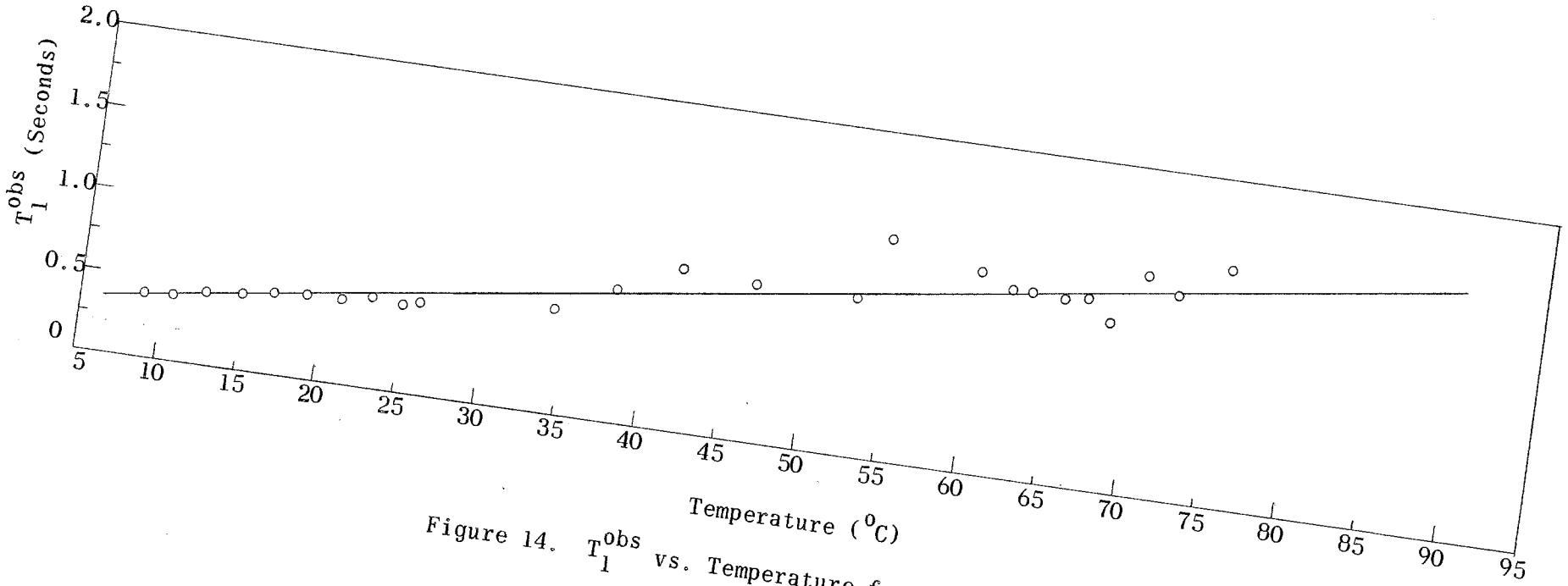

Figure 14. T_1^{obs} vs. Temperature for $MnCl_2$ Solution.

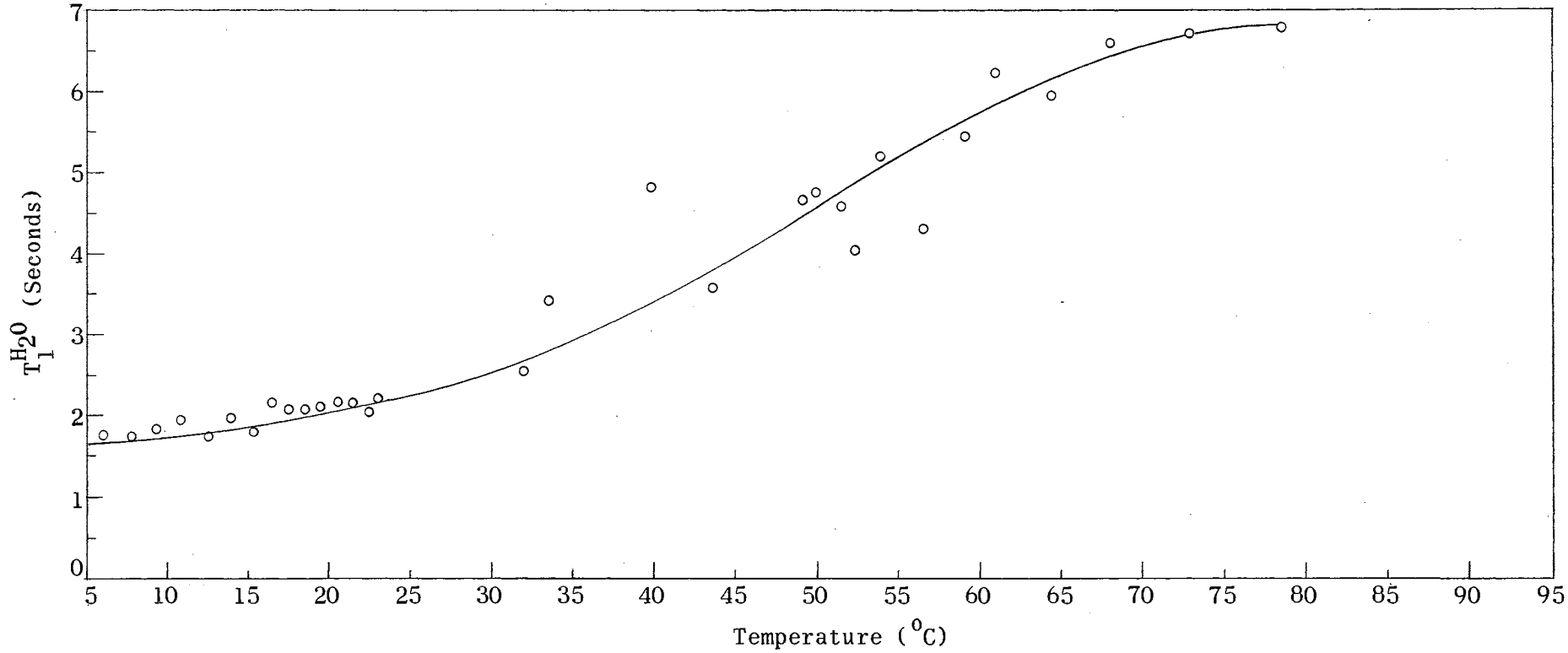

Figure 15. $T_1^{H_2O}$ vs. Temperature for Water.

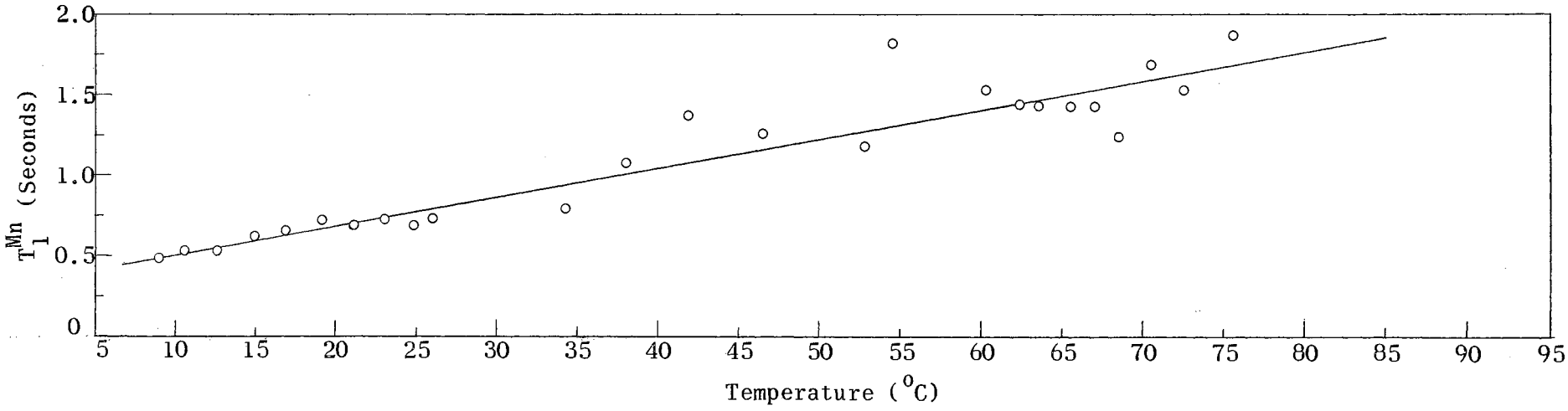

Figure 16. T_1^{Mn} vs. Temperature for $MnCl_2$ Solution.

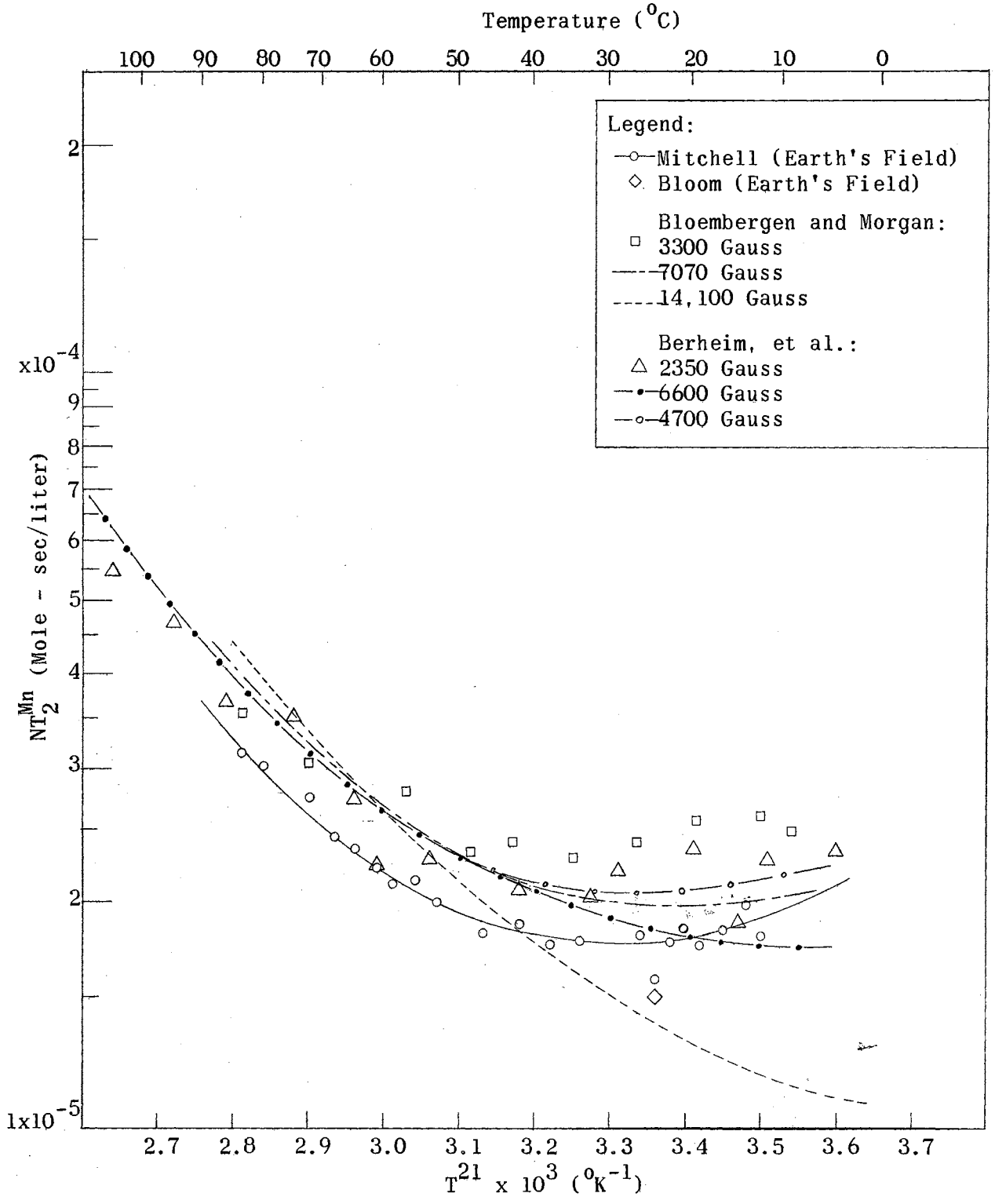

Figure 17. NT_2^{Mn} vs. Reciprocal Absolute Temperature for $MnCl_2$ Solution.

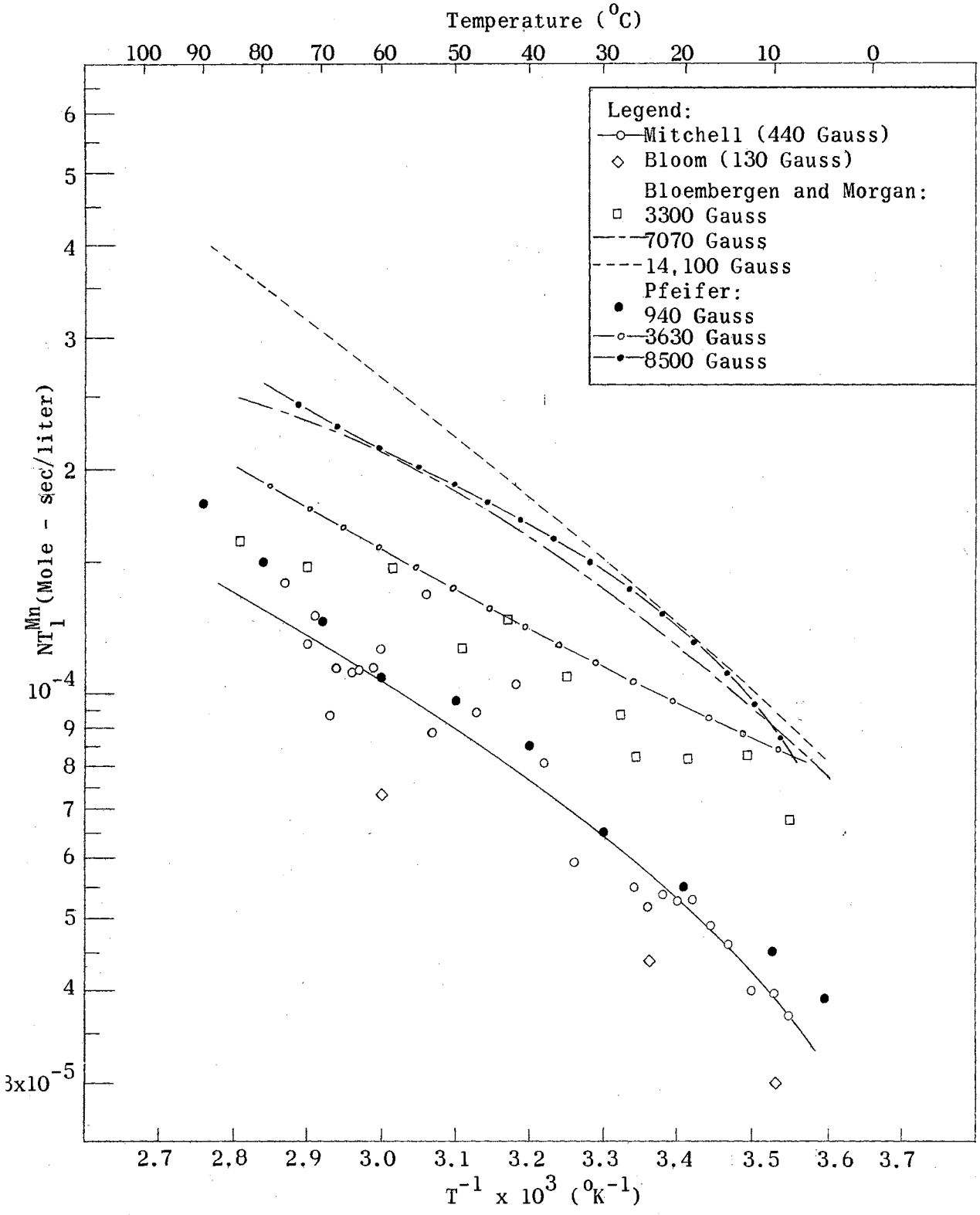

Figure 18. NT_1^{Mn} vs. Reciprocal Absolute Temperature for $MnCl_2$ Solution.

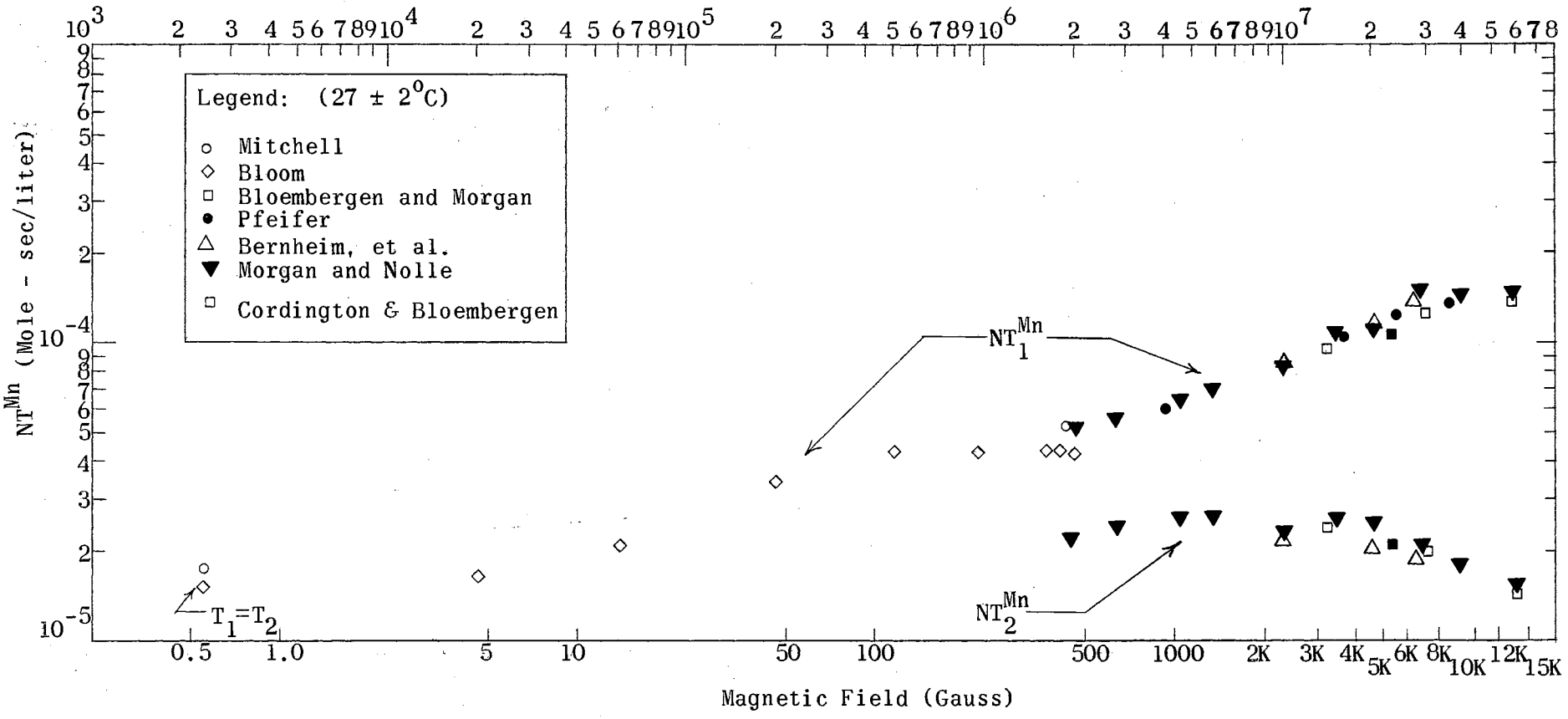

Figure 19. NT_1^{Mn} and NT_2^{Mn} vs. Magnetic Field.

of the system. The experiments performed on manganese solutions have served primarily as testimony to the successful operation of the apparatus described and the techniques for its use. It is the opinion of the experimenter that such evidence has well served as justification for the utilization of the present system as a foundation for advanced research in the field of magnetic resonance. The apparatus warrants itself in view of its relative simplicity and economy in contrast to most high field systems.

In regard to further study of the apparent implications inferred from the results on transverse relaxation times in the manganese solution, it cannot be overemphasized that reproduction of the present results is of high necessity. It is suggested, however, that further attempts to reproduce these results be carried out subsequent to several refinements in the present system. An obvious source of uncertainity in the accuracy of the final results lies in the methods of data reduction; namely, the graphical analyses for determining relaxation times leave something to be desired.

This problem cannot be completely eliminated, but considerable reduction in error is possible by incorporating a permanent image oscilloscope into the system. Such an instrument would enable more careful and hence, more accurate measurement of signal amplitudes. It would also be possible to measure the transverse relaxation time T_2 directly from observation of the decay time of the precession signal, provided sufficient signal-to-noise is available.

Methods of increasing the existing signal-to-noise warrant definite study. One immediate aid to this problem is the replacement of the existing cable between the coils and input circuit by one which is less lossy.

It is also suggested that investigations be made concerning the construction of high Q coils, particularly in the techniques for winding the coils to reduce inter-winding capacitance. This problem is no doubt a difficult one, and perhaps not justified for immediate purposes.

Further experimental study concerning field dependence of T_1 and T_2 cannot be made with the present apparatus. As pointed out in Chapter I, however, instrumentation advances are being made at the writing of this paper which will enable a more complete study of T_1 and T_2 in low and moderate fields. The necessity of this study is very important, particularly in connection with T_2, since no data is presently available in fields below 500 gauss, with the exception of the measurements in the earth's field by Bloom (6) and by those made in the present experiments. These additional refinements in the apparatus will also enable similar measurements on T_1 from which the ratio of T_2 to T_1 should be checked in weak fields to confirm the published fact that the ratio should be unity.

BIBLIOGRAPHY

1. Bloch, F., Phys. Rev., 70, 460 (1946).

2. Packard, M., R. Varian, A. Bloom, and D. Mansir, Phys. Rev., 93, 941 (1954).

3. Elliot, D. F. and R. T. Schumacher, J. Chem. Phys., 26, 1350 (1957).

4. Brown, R. J. S. and D. D. Thompson, J. Chem. Phys., 34, 1580 (1961).

5. Brown, R. J. S. and D. D. Thompson, J. Chem. Phys., 35, 1894 (1961).

6. Bloom, A. L., J. Chem. Phys., 25, 793 (1956).

7. Hausser, R. and G. Laukien, Z. Physik, Bd. 153, 394 (1959).

8. Laukien, G., Z. Naturforsch, 11a, 222 (1956).

9. Bloembergen, N. and L. O. Morgan, J. Chem. Phys., 34, 842 (1961).

10. Bernhein, R. A., T. H. Brown, H. S. Gutowsky, D. E. Woessner, J. Chem. Phys., 30, 950 (1959).

11. Pfeifer, H., Z. Naturforsch, 17a, 279 (1962).

12. Cordington, R. S. and N. Bloembergen, J. Chem. Phys., 29, 600 (1958).

13. Bloembergen, N., E. M. Purcell, and R. V. Pound, Phys. Rev., 73, 679 (1948).

14. Morgan, L. O. and A. W. Nolle, J. Chem. Phys., 31, 365 (1959).

15. Terman, E. F. Radio Engineers' Handbook. New York: McGraw-Hill, 1943, Section 2, pp. 60-64.

VITA

Don Edward Mitchell

Candidate for the Degree of

Master of Science

Thesis: APPLICATION OF THE EARTH'S FIELD FREE PRECESSION TECHNIQUE IN MEASURING TEMPERATURE DEPENDENT PROTON RELAXATION TIMES IN A DILUTE PARAMAGNETIC SOLUTION

Major Field: Physics

Biographical:

Personel Data: Born in Oklahoma City, Oklahoma, September 24, 1939, the son of Luke and Mary Mitchell.

Education: Attended grade school in Fort Smith and Little Rock, Arkansas; and high school in Little Rock, Arkansas, and Tulsa, Oklahoma; received a Bachelor of Science degree from Oklahoma State University, Stillwater, Oklahoma, in August, 1961; completed requirements for the Master of Science degree in January, 1964.

Organizations: Member of Sigma Pi Sigma and Delta Chi.